Paper ID: CE 0208

Rheological, Hardened, and Non-destructive Characteristics of Supplementary Cementitious Materials for The Production of Self-Compacting Concrete

A. Paul[1], M. H. R. Sobuz[2]

[1]Department of Building Engineering and Construction Management, KUET, Bangladesh **(paularpa98@gmail.com)**
[2] Department of Building Engineering and Construction Management, KUET, Bangladesh **(habib@becm.kuet.ac.bd)**

Abstract

Self-Compacting Concrete (SCC) typically requires a high cement content and admixtures to achieve its unique properties resulting in high production costs compared to conventional concrete. Therefore, examining methods for reducing production costs and producing cheaper SCC is prudent. This research aims to investigate the fresh and hardened properties of SCC combining steel fiber, glass powder (GP), and limestone powder (LP) and identify the optimum amount of glass powder. Steel fiber was incorporated into five concrete mixtures with GP as a 10% substitute for cement weight and LP as a replacement for 0%, 5%, 10%, 15%, and 20% of the sand, respectively. It has been demonstrated that adding supplementary cementitious material, such as limestone powder (LP) and glass powder (GP) improves the strength and workability features of SCC incorporating steel fiber. To establish the workability of fresh concrete samples, several tests like slump flow, J-ring flow and T_{50} tests were done in conformity with EN 12350. Also, the strength of hardened concrete and NDT were assessed using compressive strength and rebound hammer tests per ASTM standards. The test results demonstrated that when the GP and steel fibre amount increased, the workability and hardened properties were reduced compared to the control SCC. In 10% replacement of GP and LP produces higher strength than other replacements. So, it has been found that supplementing 10% material mixing with cement and sand yields the most benefits and can be utilized in remote construction areas.

Keywords: *Self-compacting concrete; Limestone powder; Strengt;, Workability; Steel fiber.*

1 Introduction

Self-consolidating concrete (SCC) has outstanding flowability properties in its rheological state. It also has a high resistance to segregation, which may maintain the homogeneity of concrete before and after carrying and laying Khayat (1999). SCC creates durable concrete structures while reducing labor costs and the environmental impact of consolidation. Large amounts of Portland cement increase cement consumption, result in high heat of hydration that leads to concrete cracking, have an ecological effect due to CO_2 emissions, generate energy and natural resources, and raise production costs, all of which are necessary components of an SCC mix. Mohammed et al. (2013). Incorporating supplementary cementitious materials (SCMs) as a substitute for cement can greatly reduce the production cost of SCC and alleviate the shortages of cement raw materials and solid waste pollution Wang et al. (2020).

The impact of including SCM has been the subject of numerous research into SCC mixes by replacing SCM with cement and sand, such as pulverized fuel ash and condensed silica fume, fly ash, eggshell powder, and palm oil fuel ash, fly ash (FA), metakaolin, limestone are being utilized to decrease the cost of SCC production Mounika et al. (2021). Limestone Powder is a pozzolanic substance that can be utilized as a cementitious component in concrete mixtures. By adding the mixture, the pozzolanic and filler effects of FA and LP boosted the concrete's compressive strength Khan et al. (2019). Glass aggregate is durable though brittle, possesses angular particle shapes, has a smoother surface, and has low shrinkage. Kou and Poon (2009) observed that as the amount of recycled glass in SCC combinations grew, the material's compressive strength, static modulus of elasticity, and splitting tensile strength, decreased. Tariq (2021) observes that the compressive strength of concrete decreases gradually with increasing amount of GP and the strength increases at delayed time. Numerous studies on the incorporation of steel fiber, glass fiber, polypropylene fiber and nylon is included in SCC mixtures to create high-strength fiber-reinforced concrete (FR-SCC). Abdelrazik and Khayat (2020) found that workability in the

rheological state is impacted by the incorporation of steel fibers into SCC Abdelrazik and Khayat (2020). Zemai and Shi (2015) found that adding steel fibers at 1%, 2%, and 3% reduced flowability by 14.9%, 25.6%, and 38.2%, respectively. In comparison to straight fibers, the flowability of mixes containing 1%, 2%, and 3% hooked-end steel fibers decreased by 20.9%, 35.8%, and 51.9%, respectively Wu et al. (2016). As an alternative to destructive testing, non-destructive testing Brandt (2008) has developed because of its advantages over destructive testing in terms of cost, waste, and efficiency. As the demand for natural resources increases and there is a significant increase in the production of demolition debris, waste GP has become a viable, environmentally acceptable alternative in the construction sector. Datta et al. (2022). This paper mainly attempts to incorporate steel fiber, limestone powder, and glass powder in an integrated manner to be used in SCC which has not been done yet. Day-by-day solid waste from different materials and sources increases daily, hampering the ecological habitat and biodiversity. Solid waste like limestone and glass powder in SCC can be an effective way to reduce it as they are very much available in the local and remote areas. This study aims to investigate the impact of steel fibre- and limestone-containing glass powder. Therefore, it is reasonable to examine the performance of the combined effect of materials incorporating fiber and meet the acceptance criteria for the use of combined materials on reinforcing SCC.

2 Materials

This study used ordinary Portland cement (Topçu & Canbaz) of type II, limestone powder from the local market, and silica fume from the 'NEOTECH Construction Chemical Company Ltd, Dhaka'. As coarse aggregate, natural stone chips were crushed, Kushtia-sand was used as fine aggregate, and waste glass was used as a substitute of fine aggregate. The physical parameters of the material, including fineness modulus, specific gravity, void ratio, absorption, and unit weight, were assessed following the guidelines outlined in ASTM C127-15. Table 1 shows the material physical property test outcome. The grading curve for coarse and fine aggregates produced from sieve analysis test data is shown in Figure 3. Glass typically consists of about 70.4-74.4 percent silica (SiO_2), 12.0-16.0 percent soda (Na_2O), and 10.0-15.0 percent lime Cao et al. (2017). Figure 1 and Figure 2 show the Los Angeles Abrasion Machine and Glass powder. Superplasticizers are additives used to produce concrete with high strength and fluidity mixed with potable water.

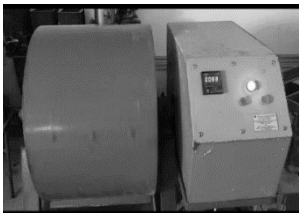

Figure 1: Los Angeles Abrasion Machine

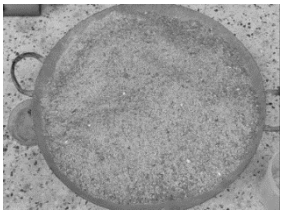

Figure 2: Glass Powder

2.1 Mixture Proportion, Concrete Mixing, Casting, and Curing of Concrete

According to the recommendations from EFNARC (2002), the research involved creating numerous trial mixtures of concrete by adjusting the amounts of superplasticizer and water-binder. By using varied percentages of LP in place of sand, five different mix patterns were used. The control mix followed the standard mix proportion of 1:1.75:1.5 for OPC, fine aggregate, and coarse aggregate. The other 4 mixes had 5%, 10%, 15%, and 20% GP substitution with a constant 10% cement replacement with sand. Table 1 shows the mix design of SCC. At first 70% water was added, and the mixture was thoroughly stirred for 2 minutes.

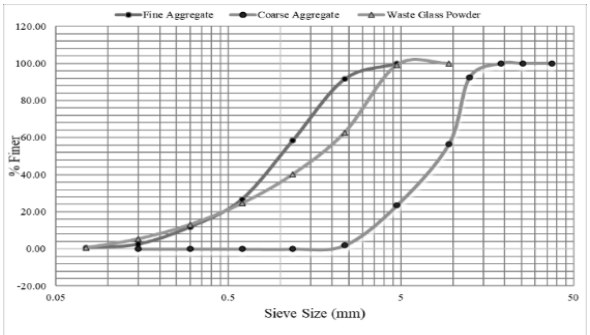

Figure 3: Grading curve of fine aggregate, coarse aggregate, and glass powder

Superplasticizer was combined with the additional 30% of the water and added to the mixture until flow was noticed. The mixing process was completed following. ASTM C192-18. Each batch of concrete's rheological characteristics were evaluated right away after mixing. After 48 hours, the molds were removed, and the specimens were numbered and cured for 7, 28, and 90 days in fully immersed conditions with potable water in curing tanks and water cured at room temperature (25 °C).

Table 1: Mix design of concrete

Mix ID	Cement (kg/m^3)	Limestone powder (kg/m^3)	Sand (kg/m^3)	Glass powder (kg/m^3)	Coarse aggregate (kg/m^3)	Silica fume (kg/m^3)	Superplasticizer (%)	Steel fiber (kg/m^3)	Water/binder (kg/m^3)
Control	300	-	525	-	450	30	1	38.54	118.8
LP10GP5	270	30	498.75	26.5	450	30	1	38.54	118.8
LP10GP10	270	30	472.5	52.5	450	30	1	38.54	118.8
LP10GP15	270	30	446.25	78.75	450	30	1	38.54	118.8
LP10GP20	270	30	420	105	450	30	1	38.54	118.8

2.2 Test Set-Up and Instrumentation

All fresh, hardened, and non-destructive concrete properties tests were conducted in the structural and material engineering laboratory of the Department of Building Engineering and Construction Management at Khulna University of Engineering and Technology in Bangladesh. These papers cover four tests: Slump flow test, J-ring test, Compressive strength test, and rebound hammer test.

The slump flow test and J-ring slump flow test were conducted according to BS EN 12350-8 (2010b), and BS EN 12350-12 (2010) was performed to evaluate the flowability and passing ability of self-compacting concrete (SCC). The sample was placed in the cone and positioned perpendicular to the base plate, with the stopwatch stopping when the front edge of the concrete reached initial contact with the 500 mm circle. The time taken to touch a 500 mm circle was recorded as T50. Figure 4 shows the slum flow test of SCC. The J-ring testing procedure was similar to slump flow tests, only differences J-ring was placed on the center of the base plate. Figure 5 shows the visual representation of the J-Ring flow test below.

Figure 4: (a) Slump cone setting, (b) Concrete mix labeling in Abram cone, (c) Slump flow measuring

Figure 5: J-Ring flow test

Figure 6: Compressive strength test

Figure 7: Rebound hammer test

The compressive test was performed according to ASTM C39 / C39M-20 (2020. The UTM had a digital configuration and a 3000 kN capacity. The specimens were extracted after curing for 7, 28, and 56 days, and excess water was removed. The specimen was centered on the machine's base plate and loaded at 0.15-0.35 MPa/s until failure. Figure 6 shows the compressive strength test setup. From failure load, compressive strength can be calculated. The rebound mallet provides a convenient and rapid evaluation of the compressive strength of concrete (1992). It consists of a spring-operated steel strike that, after released, strikes on the surface with a steel plunger. After cleaning and drying the concrete surface, the rebound hammer was held perpendicular to the surface until impact. On the screen, the compressive strength was displayed. Figure 7 depicts a visual representation of the rebound hammer test.

3 Results and Discussion

3.1 Fresh test result

Rheological tests were carried out immediately after completing uniform mixing. This study conducted fresh property tests: Slump flow and T_{50}, J-ring flow test.

3.1.1 Effect of supplementary cementitious material on Workability and Flowability of SCC

Slump flow value reduces with an increasing percentage of LP and GP. SCC mixes LP0GP0, the control mix with 0% of both LP and GP, have the highest slump flow value of 731 mm and decreased gradually with 10% limestone powder and varying glass powder amounts of 5% to 20%. LP10GP20 mix has the lowest slump flow of 675 mm. This decreasing phenomenon of the slump value can be explained by the larger absorption of water by LP and the substantially lower absorption of water by GP. Similar findings were observed by Vanjare and Mahure (2012) and Ali and Al-Tersawy (2012) that the value of decreases with increased GP. The reason is as same as of Slump flow value decreasing pattern. The highest J-ring slump flow value measured in control mix LP0GP0 is 722 mm, which is nearly identical to slump flow test value (731 mm) for the same mix. The average flow diameter as per EFARNAC was found to be 550 mm. Figure 8 shows the slump flow and J-ring slump flow for different SCC mixtures.

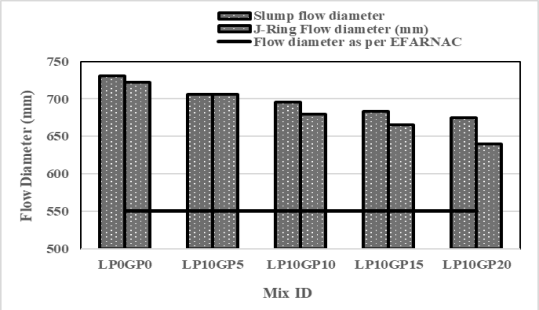

Figure 8: Slump flow value of SCC with varying glass percentage

The time needed for the flowing increased with the decrease in slump flow value. So, the time required for slump to reach the 500 mm “T50” increased with the constant percentage of LP and increasing percentage of GP.

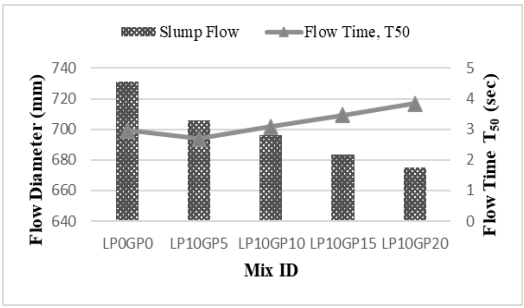

Figure 9: Slump flow and T_{50} time for different types of SCC mix

Slump flow time T_{50} was observed to be highest for the control mix LP10GP20 is 3.84 sec and minimum for the control mix LP10GP5 is 2.69 sec. This time has decreased slightly from the control mix with no LP and GP of value 2.96 sec to 2.69 sec when 10% LP and 5% GP were added in SCC Figure 9 shows that T_{50} value to the slump flow value for various mixes.

3.1.2 Effect of supplementary cementitious material on the Passing Ability of SCC

The highest J-ring flow measurement for the control mix LP0GP0 is 722 mm, which is nearly identical to the result of the slump flow test (731 mm). Thus, it may be concluded that the control mix does not contain such blocking. The determined blocking index of the above-mentioned control combination was 12.5. The blocking index for LP10GP5, LP10GP10, LP10GP15, and LP10GP20 was 27.5, 32.5, 30, and 42.5, respectively. The blocking index increased from LP10GP5 to LP10GP10, then decreased slightly in the control mix LP10GP15 and again increased in the case of control mix LP10GP20. This result indicates that there is a decreasing pattern in passing ability with the constant 10% LP and increasing percentage of GP. Rehman et al. (2018) found that the increases of GP decrease even though all SCC mixtures showed acceptable passing ability characteristics due to the slump value falling within the 550–750 mm range established by EFNARC for SCC acceptance requirements. The findings show that the SCC mixes created for this investigation had the appropriate passing ability and maintained a high level of segregation resistance. Figure 10 shows slump flow, blocking index, and J-ring flow for several SCC combinations.

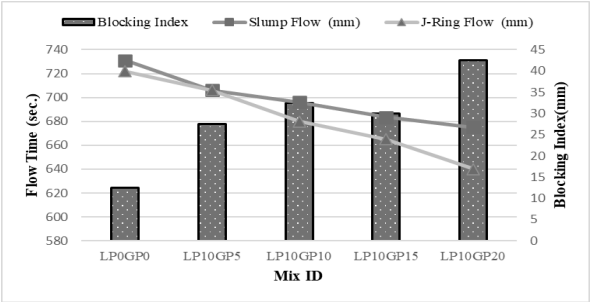

Figure 10: J-ring flow, Slump flow, and Blocking index for different types of SCC mix

3.2 Hardened and NDT test results

3.2.1 Compressive strength test

The figure shows all cylindrical specimen compressive strength test results. Averaging three samples gave each composition's mean compressive strength. Each concrete sample shows compressive strength, averages, standard deviations, coefficients of variation, standard errors, 95% confidence intervals (MIs), and margins of error. The compressive strength of the material is displayed in Figure 11 at 7, 28, and 56 days from 23.485 MPa to 38.867 MPa. At 56 days, LP0GP0 exhibited the highest mean compressive strength of 38.865 MPa with a 95% confidence interval of 33.583 and 44.147 MPa. LP10GP20 had the lowest mean compressive strength at 28 days, 23.42 MPa. The LP0GP0 control mix with 0% substitution of supplementary cementitious materials had mean compressive strengths of 31.32 MPa, 33.34 MPa, and 38.865 MPa at 7, 28, and 56 days. At 7, 28, and 56 days, the LP10GP10 mix had 28.12 MPa, 30.02 MPa, and 32.115 MPa, respectively. At 56 days, the LP10GP10 mix exhibited the second-highest mean compressive strength of 32,115 MPa. Rehman et al. (2018) found that compressive strength decreases with increased GP. Rajathi and Portchejian (2014) show opposition as the strength increases with an increasing amount of GP. The compressive strength of different concrete mixes at 7, 28, and 56 days is shown in Figure 11 below.

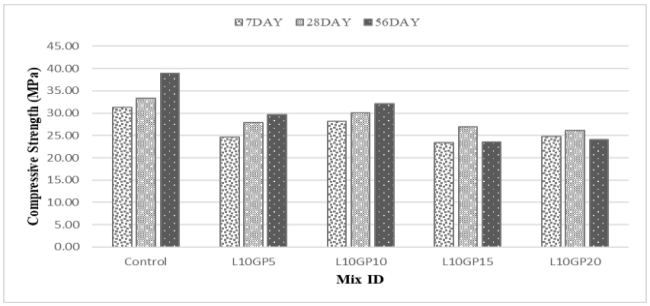

Figure 11: Compressive strength of different concrete mix at 7,28,56 day

In the mix, LP10GP15 and LP10GP20 have a lower strength in 56 days than in 28 days. That happened due to shrinkage and micro-structural cracks appearing in the concrete. The strength decreases with increased GP due to a lower bond between cement and glass powder. The bond between glass powder surface and cement is not as good as the bond with sand. Strength is decreased because the cement's cohesiveness with the glass surface is lower than that of the cement's matrix with sand.

3.2.2 Rebound Hammer Test

The rebound hammer test is an effective and feasible non-destructive method for evaluating concrete compressive strength using rebound index (rebound number). The rebound number is a measurement of surface hardness. Figure 12 shows the rebound hammer test conducted using a variable amount of supplementary cementitious material on specimens collected at 28 and 56 days. The control samples' average rebound hammer index values range from 23 MPa to 30 MPa. In contrast, the rebound index values for the various concentrations of limestone powder and glass powder with samples ranged from 24.6 MPa to 30.7 MPa. The rebound hammer test outcome is that the strength increases with increased GP Singh and Singh (2018). The rebound hammer strength of mix LP10GP10 is higher than other mixes without control mix, which is relative to the compressive strength of the destructive test, and the mix bond is stronger than other mixes. Figure 12 shows the rebound hammer test result for different concrete mixes at 28 and 56 days.

.

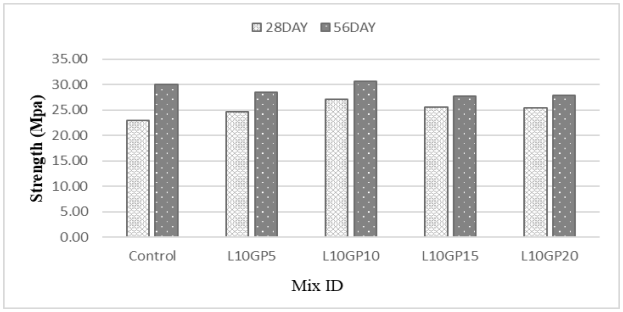

Figure 12: Rebound hammer test result for the different concrete mix at 28 and 56 days

4 Conclusion and Recommendation

The important findings from the research are as follows:

- It can be concluded that slump and J-ring flow decrease with an increasing percentage of GP, including LP and Steel fiber. The values were within the EFNARC range, suggesting appropriate workability, passing ability, and flow ability.
- In the case of the compressive strength test, LP10GP10 has given the better result among other percentages of GP mixes.
- Rebound hammer tests were qualitative, and mixes showed good surface hardness. LP10GP10 yielded the best results for 10% partially replaced GP with LP and steel fiber concrete.

References

Abdelrazik, A. T., & Khayat, K. H. (2020). Effect of fiber characteristics on fresh properties of fiber-reinforced concrete with adapted rheology. Construction and Building Materials, 230, 116852.

Ali, E. E., & Al-Tersawy, S. H. (2012). Recycled glass as a partial replacement for fine aggregate in self compacting concrete. Construction and Building Materials, 35, 785-791. https://doi.org/https://doi.org/10.1016/j.conbuildmat.2012.04.117

Brandt, A. M. (2008). Fibre reinforced cement-based (FRC) composites after over 40 years of development in building and civil engineering. Composite structures, 86(1-3), 3-9.

Cao, Q., Cheng, Y., Cao, M., & Gao, Q. (2017). Workability, strength and shrinkage of fiber reinforced expansive self-consolidating concrete. Construction and Building Materials., 131, 178-185.

Datta, S. D., Sobuz, M. H. R., Akid, A. S. M., & Islam, S. (2022). Influence of coarse aggregate size and content on the properties of recycled aggregate concrete using non-destructive testing methods. Journal of Building Engineering, 61, 105249.

Khan, M. I., Usman, M., Rizwan, S. A., & Hanif, A. (2019). Self-Consolidating Lightweight Concrete Incorporating Limestone Powder and Fly Ash as Supplementary Cementing Material. Materials, 12(18), 3050. https://www.mdpi.com/1996-1944/12/18/3050

Khayat, K. H. (1999). Workability, testing, and performance of self-consolidating concrete. Materials Journal, 96(3), 346-353.

Mohammed, M. K., Dawson, A. R., & Thom, N. H. (2013). Production, microstructure and hydration of sustainable self-compacting concrete with different types of filler. Construction and Building Materials, 49, 84-92. https://doi.org/https://doi.org/10.1016/j.conbuildmat.2013.07.107

Mounika, G., Baskar, R., & Sri Kalyana Rama, J. (2021). Rice husk ash as a potential supplementary cementitious material in concrete solution towards sustainable construction. Innovative Infrastructure Solutions, 7(1), 51. https://doi.org/10.1007/s41062-021-00643-5

Rajathi, A., & Portchejian, G. (2014). Experimental study on self compacting concrete using glass powder. Int J Struct Civ Eng Res, 3(3), 73-79.

Rehman, S., Iqbal, S., & Ali, A. (2018). Combined influence of glass powder and granular steel slag on fresh and mechanical properties of self-compacting concrete. Construction and Building Materials, 178, 153-160. https://doi.org/https://doi.org/10.1016/j.conbuildmat.2018.05.148

Singh, N., & Singh, S. (2018). Evaluating the performance of self compacting concretes made with recycled coarse and fine aggregates using non destructive testing techniques. Construction and Building Materials, 181, 73-84.

Topçu, İ. B., & Canbaz, M. (2004). Properties of concrete containing waste glass. Cement and Concrete Research, 34(2), 267-274. https://doi.org/https://doi.org/10.1016/j.cemconres.2003.07.003

Vanjare, M. B., & Mahure, S. H. (2012). Experimental investigation on self compacting concrete using glass powder. International Journal of Engineering Research and Applications (IJERA), 2(3), 1488-1492.

Wang, D., Wang, Q., & Xue, J. (2020). Reuse of hazardous electrolytic manganese residue: Detailed leaching characterization and novel application as a cementitious material. Resources, Conservation and Recycling, 154, 104645.

Wu, Z., Shi, C., He, W., & Wu, L. (2016). Effects of steel fiber content and shape on mechanical properties of ultra high performance concrete. Construction and Building Materials, 103, 8-14. https://doi.org/https://doi.org/10.1016/j.conbuildmat.2015.11.028